Real-Time Observation of Plasma Protein Film Formation on Well-Defined Surfaces with Scanning Force Microscopy

Truong C. Ta, Michael T. Sykes, and Mark T. McDermott*

Department of Chemistry, University of Alberta, Edmonton, AB T6G 2G2 Canada

Received November 13, 1997. In Final Form: February 10, 1998

We report here the results of a scanning force microscopic (SFM) investigation into the structure of adsorbed bovine fibrinogen films on well-defined surfaces. SFM images show that a monolayer of fibrinogen assembles on both highly oriented pyrolytic graphite (HOPG) and mica. We find, however, that the film morphology varies as a function of the substrate. To unravel the nature of the observed differences, we tracked the growth of bovine fibrinogen layers at both surfaces in real-time. Consistent with the differences observed in the final film structure, we find that film formation on HOPG and mica proceeds through distinct mechanisms. A network is observed during fibrinogen film formation on HOPG, implying that protein−protein interactions are involved in the growth mechanism and likely govern the final film structure. The growth mechanism on mica proceeds by the homogeneous increase in the number of nuclei across the surface and gives no indication of significant intermolecular interactions. Surfactant elution studies show that films on HOPG are more tightly bound than those on mica, as predicted on the basis of the observed growth mechanisms. An adsorption mechanism consistent with our observations and based on the known structure of fibrinogen is proposed.

Introduction

The importance of adsorbed protein films to areas such as implant medicine, biosensor design, food processing, and chromatographic separations has provided the incentive for researchers from a broad range of disciplines to focus studies on protein−surface interactions.[1] When a foreign material comes into contact with blood, it is generally accepted that a complex biomolecular film forms rapidly at the interface. Important components of this film include plasma proteins which are involved in the blood-clotting cascade and have also been shown to modify the interaction of various blood components at the blood−biomaterial interface.[2] Numerous studies have lead to the general understanding that the type, amount, and conformation of surface-bound plasma proteins are all crucial in determining the biocompatibility of materials.[1,3,4]

Fibrinogen (FG) is one plasma protein that has received much attention due to its dual functionality in thrombosis (formation of a blood clot). The conversion of FG to fibrin and the subsequent polymerization of fibrin is a key step in blood clot formation. Fibrinogen also serves as an adhesive agent in the aggregation of platelets, which occurs simultaneously with fibrin polymerization in the development of a hemostatic blood clot.[5] A variety of techniques have been employed to probe the interfacial properties of FG including ellipsometry,[6] infrared spectroscopy,[7] radio labeling,[8] surface plasmon resonance,[9] and X-ray photoelectron spectroscopy.[10] These methodologies have provided a wealth of macroscopic information reflecting behavior averaged over the entire surface. The structure of single FG proteins[11] and the architecture of FG films[12] have also been probed at microscopic length scales in scanning electron microscopy (SEM) investigations. Recently, immunogold labeling combined with SEM imaging has been utilized to probe the architecture of adsorbed FG films.[13] The results of both macroscopic and microscopic studies to date have shown that FG binds strongly and in high amounts to most surfaces and competes

* To whom correspondence should be addressed. Voice: 403-492-3687. Fax: 403-492-8231. E-mail: mark.mcdermott@ualberta.ca.

(1) (a) Brash, J. L., Horbett, T. A., Eds. *Proteins at Interfaces: Physiochemical and Biochemical Studies*; ACS Symposium Series No. 343; American Chemical Society: Washington, DC, 1986. (b) Horbett, T. A., Brash, J. L., Eds. *Proteins at Interfaces II: Fundamentals and Applications*; ACS Symposium Series No. 602; American Chemical Society: Washington, DC, 1995.

(2) Morrissey, B. W. *Ann. N. Y. Acad. Sci.* **1977**, *283*, 50−64.

(3) (a) Andrade, J. D.; Hlady, V. *Ann. N. Y. Acad. Sci.* **1987**, *516*, 158−72. (b) Horbett, T. A. *Cardiovasc. Pathol.* **1993**, *2*, 137S−148S.

(4) Feng, L.; Andrade, J. D. In *Proteins at Interfaces II: Fundamentals and Applications*; Brash, J. L., Horbett, T. A., Eds.; ACS Symposium Series No. 602; American Chemical Society: Washington, DC, 1995; Chapter 5.

(5) See ref 4 and references therein.

(6) See, for example: (a) Andrade, J. D., Ed. *Surface and Interfacial Aspects of Biomedical Polymers*; Plenum Press: New York, 1985; Vols. 1 and 2. (b) Prime, K. L.; Whitesides, G. M. *Science* **1991**, *252*, 1164−7.

(7) (a) Lenk, T. J.; Chittur, K. K.; Ratner, B. D. *Trans. Soc. Biomater.* **1989**, *15*, 134. (b) Chittur, K. K.; Fink, D. J.; Hutson, T. B.; Gendreau, R. M.; Jakobsen, R. J.; Leininger, R. I. In *Proteins at Interfaces: Physiochemical and Biochemical Studies*; Brash, J. L., Horbett, T. A., Eds.; ACS Symposium Series No. 343; American Chemical Society: Washington, DC, 1986; Chapter 23.

(8) See, for example: (a) Ward, C. A.; Stanga, D. *J. Colloid Interface Sci.* **1986**, *114*, 323−29. (b) Lahav, J. *J. Colloid Interface Sci.* **1987**, *119*, 262−74. (c) Young, B. R.; Pitt, W. G.; Cooper, S. L. *J. Colloid Interface Sci.* **1988**, *125*, 246−60.

(9) (a) Mrksich, M.; Sigal, G. B.; Whitesides, G. M. *Langmuir* **1995**, *11*, 4383−5. (b) Green, R. J.; Davies, J.; Davies, M. C.; Roberts, C. J.; Tendler, S. J. B. *Biomaterials* **1997**, *18*, 405−13.

(10) Ratner, B. D.; McElroy, B. J. In *Spectroscopy in the Biomedical Sciences*; Gendreau, R. M., Ed.; CRC Press Inc.: Boca Raton, FL, 1986; pp 107−140.

(11) (a) Hall, C. E.; Slayter, H. S. *J. Biophys. Biochem. Cytol.* **1959**, *5*, 11. (b) Gorman, R. R.; Stoner, G. E.; Catlin, A. *J. Phys. Chem.* **1971**, *75*, 2103−7. (c) Fowler, W. E.; Erickson, H. P. *J. Mol. Biol.* **1979**, *134*, 241−9.

(12) (a) Köppel, G. *Z. Zellforsch.* **1967**, *77*, 443−517. (b) Stoner, G. E.; Srinivasan, S.; Gileadi, E. *J. Phys. Chem.* **1971**, *75*, 2107−11. (c) Rudee, M. L.; Price, Y. M. *J. Biomed. Mater. Res.* **1985**, *19*, 57−66. (d) Brynda, E.; Houska, M.; Lednocky, F. *J. Colloid Interface Sci.* **1986**, *113*, 164−71. (e) Nygren, H.; Stenberg, M. *J. Biomed. Mater. Res.* **1988**, *22*, 1−11. (f) Eberhart, R. C.; Munro, M. S.; Frautschi, J. R.; Sevastianov, V. I. In *Proteins at Interfaces: Physiochemical and Biochemical Studies*; Brash, J. L., Horbett, T. A., Eds.; ACS Symposium Series No. 343; American Chemical Society: Washington, DC, 1986; Chapter 24.

(13) (a) Park, K.; Albrecht, R. M.; Simmons, S. R.; Cooper, S. L. *J. Colloid Interface Sci.* **1986**, *111*, 197−212. (b) Murthy, K. D.; Diwan, A. R.; Simmons, S. R.; Albrecht, R. M.; Cooper, S. L. *Scanning Microsc.* **1987**, *1*, 765−73. (c) Pankowsky, D. A.; Ziats, N. P.; Topham, N. S.; Ratnoff, O. D.; Anderson, J. M. *J. Vasc. Sur.* **1990**, *11*, 599−606.

S0743-7463(97)01234-1 CCC: $15.00
Published on Web 04/09/1998

efficiently with other proteins for adsorption sites.[4] Although this knowledge has provided some insights into the factors affecting blood biocompatibility, the nature of fibrinogen's high surface activity is not completely understood.

Relative to the cases for other proteins, the amount of FG adsorbed is less sensitive to substrate composition.[4] Because of this low substrate influence, the presence of a dense FG film at the solution−biomaterial interface is not an absolute indicator of the material's biocompatibility. A factor which is likely important in determining thromboresistance is the conformation of the surface-bound FG. For example, platelet adhesion correlates with factors other than the total amount of FG adsorbed, suggesting that the orientation of the adsorbed FG is significant.[14] A number of parameters have been shown to influence the conformation of adsorbed FG, including the nature of the substrate[12c,15] and the concentration of FG in solution before adsorption.[15c,16] There is also evidence for post-adsorptive transitions in the FG structure,[17] which highlights the complexity of FG interfacial interactions. Common methods employed to probe the conformation of FG in adsorbed films are generally indirect, involving observation of the protein's ability to bind platelets[14,17a] and antibodies[14a,d,17a,18] or measuring the amount of protein that is eluted from the surface by a surfactant such as sodium dodecyl sulfate (SDS).[18,19] Spectroscopic techniques such as infrared spectroscopy[7] and circular dichroism[20] have also been utilized to probe conformational changes in protein layers. These techniques have advanced our understanding of the factors that affect preformed FG films; however, little information exists on the initial growth process of FG layers and the influence of the substrate on growth mechanisms. The mechanism of FG film formation is of interest because the manner in which an adsorbed layer forms directly influences the structure and properties of the completed film.

Early studies focused on the initial growth of FG layers generally involved measuring the amount of FG adsorbed as a function of time or solution concentration (adsorption isotherms).[8,21] These investigations have shown that FG adsorption is rapid and yields isotherms generally exhibiting a saturation plateau reflecting a closely packed monolayer. The saturation coverage varies slightly from surface to surface, implying surface-induced conformational changes or varying amounts of protein−protein interactions.[21] Microscopic studies of the initial stages of FG adsorption have been carried out by SEM imaging of films adsorbed from solutions of varying concentration[12e] or of samples where film formation had been interrupted at various times (quenched films).[12c] These investigations also involved staining of the quenched films to provide contrast for SEM imaging. The uncertainty in the relationship between a stained, quenched film and the actual layer forming in solution has led us to believe that an in situ, real-time observation of film growth will provide additional insights into the structure of adsorbed FG.

Scanning force microscopy (SFM) has recently found widespread use in probing biological materials.[22] The dramatic increase in popularity of SFM for examining biological systems stems from its ability to image in buffer solutions where physiological conditions such as pH, ionic strength, and temperature can be simulated. This capability has prompted the SFM observation of several biological processes in real-time. For example, a fascinating early demonstration was the real-time observation of the transformation of FG to fibrin.[23] Other examples of biological processes that have been examined in real-time include protein crystal growth[24] and the dynamic release of protein from a biodegrading polymer.[25] Individual protein dynamics have also been observed.[26]

The adsorption of plasma proteins has been probed with SFM in both static[27−29] and dynamic modes.[30] Individual FG molecules[27a] and FG films[27−29] have been imaged after the substrate had reached equilibrium with the protein solution. The real-time examination of immunoglobulin G (IgG) adsorption to mica[30a] and graphite[30b] has appeared in separate reports. The mechanism of IgG adsorption appears to vary at each substrate, providing a basis for further SFM investigations aimed at unraveling the effect of substrate on protein film growth. However, to our knowledge, SFM imaging has not been exploited to probe the initial stages of FG film growth or in the investigation of surface-induced variations of FG film structure.

We report here the results of an SFM investigation focused on the influence of substrate on the assembly of FG films. We present images detailing both preformed layers and the real-time assembly of FG films on highly oriented pyrolytic graphite (HOPG) and mica surfaces. Although these are well-defined substrates, they effectively serve as models for more complex hydrophobic and hydrophilic surfaces. Graphitic substrates are also directly relevant to biocompatibility studies due to the

(14) (a) Lindon, J. N.; McManama, G.; Kushner, L.; Merrill, E. W.; Salzman, E. W. *Blood* **1986**, *68*, 355−62. (b) Salzman, E. W.; Lindon, J.; McNamana, G.; Ware, J. W. *Ann. N. Y. Acad. Sci.* **1987**, *516*, 184−95. (c) Chinn, J. A.; Horbett, T. A.; Ratner, B. D. *Thromb. Haemostasis* **1991**, *65*, 608−17. (d) Kiaei, D.; Hoffman, A. S.; Horbett, T. A.; Lew, K. R. *Biomaterials* **1995**, *29*, 729−39.

(15) (a) Horbett, T. A *J. Biomed. Mater. Res.* **1981**, *15*, 673−95. (b) Uniyal, S.; Brash, J. L. *Thromb. Haemostasis* **1982**, *47*, 285−90. (c) Slack, S. M.; Horbett, T. A. *J. Colloid Interface Sci.* **1989**, *13*, 148−65.

(16) Slack, S. M.; Horbett, T. A. *J. Colloid Interface Sci.* **1988**, *124*, 535−51.

(17) (a) Chinn, J. A.; Posso, S. E.; Horbett, T. A.; Ratner, B. D. *J. Biomed. Mater. Res.* **1991**, *25*, 535−55. (b) Rapoza, R. J.; Horbett, T. A *J. Biomed. Mater. Res.* **1990**, *24*, 1263−87.

(18) See, for example: Horbett, T. A.; Lew, K. R. *J. Biomater. Sci., Polym. Ed.* **1994**, *6*, 15−33.

(19) (a) Bohnert, J. A.; Horbett, T. A. *J. Colloid Interface Sci.* **1986**, *111*, 363−80. (b) Rapoza, R. J.; Horbett, T. A. *J. Biomater. Sci.* **1989**, *1*, 69−80.

(20) McMillin, C. R.; Walton, A. G. *J. Colloid Interface Sci.* **1974**, *48*, 345−9.

(21) Brash, J. L. In *Proteins at Interfaces: Physiochemical and Biochemical Studies*; Brash, J. L., Horbett, T. A., Eds.; ACS Symposium Series No. 343; American Chemical Society: Washington, DC, 1986; Chapter 30.

(22) For a recent review, see: Hansma, H.; Hoh, J. H. *Annu. Rev. Biophys. Biomol. Struct.* **1994**, *23*, 115−39.

(23) Drake, B.; Prater, C. B.; Weisenhorn, A. L.; Gould, S. A.; Albrect, T. R.; Quate, C. F.; Cannell, D. S.; Hansma, H. G.; Hansma, P. K. *Science* **1989**, *243*, 1586−9.

(24) (a) Land, T. A.; Malkin, A. J.; Kuznetsov, Y. G.; McPherson, A.; Yoreo, J. J. *Phys. Rev. Lett.* **1995**, *75*, 2774−7. (b) Malkin, A. J.; Land, T. A.; Kuznetsov, Y. G.; McPherson, A.; Yoreo, J. J. *Phys. Rev. Lett.* **1995**, *75*, 2778−81.

(25) Shakesheff, K. M.; Davies, M. C.; Heller, J.; Roberts, C. J.; Tendler, S. J. B.; Williams, P. M. *Langmuir* **1995**, *11*, 2547−53.

(26) (a) Radmacher, M.; Fritz, M.; Hansma, H. G.; Hansma, P. K. *Science* **1994**, *265*, 1577−9. (b) Lewis, A.; Rousso, I.; Khachatryan, E.; Brodsky, I.; Lieberman, K.; Sheves, M. *Biophys. J.* **1996**, *70*, 2380−4.

(27) (a) Wigren, R.; Elwing, H.; Erlandsson, R.; Welin, S.; Lundström, I. *FEBS Lett.* **1991**, *280*, 225−8. (b) Rasmusson, J. R.; Erlandson, R.; Salaneck, W. R.; Schott, M.; Clark, D. T.; Lundström, I. *Scanning Microsc.* **1994**, *8*, 481−90.

(28) (a) Lea, A. S.; Pungor, A.; Hlady, V.; Andrade, J. D.; Herron, J. N.; Voss, E. W., Jr. *Langmuir* **1992**, *8*, 68−73. (b) Warkentin, P.; Wälivaara, B.; Lundström, I.; Tengvall, P. *Biomaterials* **1994**, *15*, 786−795.

(29) (a) Eppell, S. J.; Zypman, F. R.; Marchant, R. E. *Langmuir* **1993**, *9*, 2281−9. (b) Siedlecki, C. A.; Eppell, S. J.; Marchant, R. E. *J. Biomed. Mater. Res.* **1994**, *28*, 971−80. (c) Eppel, S. J.; Simmons, S. R.; Albrecht, R. M.; Marchant, R. E. *Biophys. J.* **1995**, *68*, 671−80.

(30) (a) Lin, J. N.; Lea, A. S.; Hansma, P. K.; Andrade, J. D. *Langmuir* **1990**, *6*, 509−11. (b) Cullen, D. C.; Lowe, C. R. *J. Colloid Interface Sci.* **1994**, *166*, 102−8.

use of pyrolytic carbon in prosthetic heart valves. A series of studies has recently appeared highlighting the adsorption of FG at low-temperature isotropic carbon (LTIC) surfaces.[31,32] In this study, we also utilize frictional contrast to develop insights into the structure of adsorbed protein.[30b] Our results show that the growth process observed at each substrate governs the final film properties. The details provided by our observations allow us to provide a structural basis for substrate-dependent differences in bovine fibrinogen (BFG) adsorption.

Experimental Section

Reagents and Materials. Fraction I bovine fibrinogen (BFG) with 89% clottable protein was obtained from Sigma (St. Louis, MO) and used as received. Water from a Nanopure (Barnstead, Dubuque, IA) purification system was used in all solution preparations. BFG solutions (50 μg/mL) were made in 10 mM phosphate buffer (PB) at pH = 7.4. Fibrinogen and protein-free PB solutions were filtered using a 0.22 μm millex-GV, low-protein-binding filter (Millipore, Bedford, MA) before adsorption experiments. Elution of proteins was performed with 3% w/v SDS in water. Fresh surfaces of highly oriented pyrolytic graphite (HOPG) (Advanced Ceramic Materials, Lakewood, OH) were generated by cleaving with sticky tape before each experiment. Mica (Asheville Schoonmaker Mica Co., Newport News, VA) was cleaved with a razor blade.

SFM Imaging. SFM images were obtained with a Nanoscope III (Digital Instruments, Santa Barbara, CA) equipped with a fluid cell. Silicon nitride cantilevers (Digital Instruments) with nominal spring constants of 0.06 N/m were used. For all experiments discussed here, the imaging force was $\leq$1 nN. Images are presented without filtering. A software planefit was used where necessary.

Each experiment began with the introduction of phosphate buffer into the fluid cell that was then allowed to equilibrate for 30−60 min to reduce drift. Images of the substrate in buffer were collected in order to compare the surface before and after the addition of BFG. Imaging was performed under static solution or with solution flowing through the fluid cell. For static imaging, after equilibration of the cell in PB, BFG solution was introduced into the fluid cell by a negative pressure gradient. Adsorption times were approximately 30 min. Images were taken with BFG solution in the cell and after the cell was further flushed with phosphate buffer with no apparent differences observed. Therefore, we assume that protein adsorption to the probe tip does not influence the quality of the images obtained at the resolution employed here (micron scale).

The setup for flowing solution through the SFM fluid cell is similar to that described in a previous report.[33] A 5-mL syringe body served as a reservoir for buffer and BFG solutions to be gravity fed into the fluid cell. Images were taken with the buffer solution flowing at 0.6−0.8 mL/min. When the images appeared stable, PB was allowed to flow until the syringe reservoir approached emptiness. A 50 μg/mL BFG solution was then added to the syringe reservoir, and BFG was carried into the cell by a continuous flow. Images were captured continuously at a scan rate of 10.2 Hz.

Elution Experiments. The SDS elution experiments were performed on preformed BFG films at HOPG as described for the static imaging conditions above. The BFG was equilibrated with the surface for 30 min. The 3% SDS solution was then flowed through the fluid cell for 60 min at a flow rate of ~1 mL/min. After this time, the cell was flushed with PB. Flow was stopped and images were taken in static buffer.

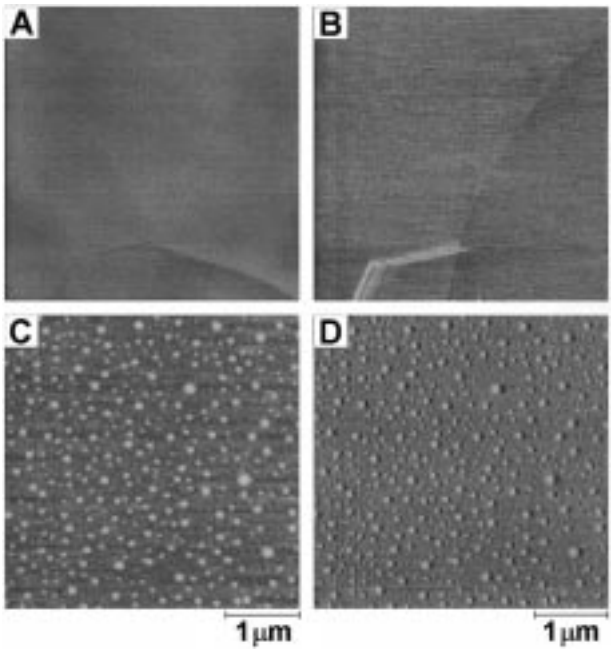

Figure 1. In situ SFM images of an unmodified HOPG substrate and a BFG film on HOPG. (A) 4 × 4 μm^2 topographic SFM image of cleaved HOPG in phosphate buffer (*z*-scale = 5 nm) and (B) corresponding lateral force image (*z*-scale = 0.1 V). (C) 4 × 4 μm^2 topographic image of a BFG film on HOPG adsorbed from a 50 μg/mL BFG solution for 30 min (*z*-scale = 20 nm) and (D) corresponding lateral force image (*z*-scale = 0.1 V).

Results and Discussion

The following sections detail our in situ topographic and lateral force SFM studies of BFG films on HOPG and mica surfaces. We first present images of BFG films preformed from 50 μg/mL solutions in PB. We designate these types of BFG layers as equilibrium films in that the surface-bound species has reached equilibrium with the solution. We then present the results of our real-time exploration of BFG film growth on the different surfaces. Last, we provide insights into surface-induced variations in final film structure through the SFM analysis of SDS elution experiments and provide a detailed model of BFG binding based on structural considerations.

Equilibrium BFG Film Structure. An illustration of the utility of SFM to probe surface-induced variations in adsorbed BFG film structure is provided by in situ images of preformed layers. The substrates utilized in the present study were thoroughly characterized before protein adsorption due a previous study which reported similarities between substrate features and biological molecules.[34] Parts A and B of Figure 1 are respective 4 × 4 μm^2 topographic and lateral force images representative of cleaved HOPG collected in PB solution. The topographic features in Figure 1A are similar to those noted in numerous SPM studies of HOPG.[35,36] The majority of the image consists of atomically flat basal plane graphite, which exhibits a relatively constant lateral force signal in Figure 1B.[36] A cleavage step is apparent in the lower portion of the image, exhibiting a lateral force signature consistent with "tripping" of the tip over the

(31) (a) Feng, L.; Andrade, J. D. *J. Biomed. Mater. Res.* **1994**, *28*, 735. (b) Feng, L.; Andrade, J. D. *J. Colloid Interface Sci.* **1994**, *166*, 419−26. (c) Feng, L.; Andrade, J. D. *Biomaterials* **1994**, *15*, 323−33.

(32) Chinn, J. A.; Phillips, R. E., Jr.; Lew, K. R.; Horbett, T. A. *J. Colloid Interface Sci.* **1996**, *184*, 11−19.

(33) Thomson, N. H.; Kasas, S.; Smith, B.; Hansma, H. G.; Hansma, P. K. *Langmuir* **1996**, *12*, 5905−8.

(34) Clemmer, C. R.; Beebe, T. P., Jr. *Science* **1991**, *251*, 640−2.

(35) See, for example: (a) Chang, H.; Bard, A. J. *Langmuir* **1991**, *7*, 1143−53. (b) McDermott, M. T.; McCreery, R. L. *Langmuir* **1994**, *10*, 4307−14.

(36) Baselt, D. R.; Baldeschwieler, J. D. *J. Vac. Sci. Technol. B* **1992**, *10*, 2316−22.

face of the step.[36,37] Generally, the surface structure of HOPG in PB imaged during this study consisted of an atomically flat basal plane and some cleavage step defects.

Exposure of the cleaved basal plane HOPG to a 50 μg/mL BFG solution results in a surface such as that depicted in Figure 1C and D. Part C of Figure 1 is a 4×4 μm^2 topographic image collected in the BFG/PB solution after 30 min of equilibration time. Figure 1D is the corresponding lateral force image. These images are clearly distinct from the images of unmodified HOPG in PB. The topography consists of uniformly dispersed spherical structures exhibiting a range of heights between 6 and 13 nm at a density of 24 ± 2 structures/μm^2.[38] We have observed spherical structures with heights up to 60 nm, and our continuing investigations have revealed that both the density and height of these structures are concentration- and flow-rate-dependent.[39] Concentration-dependent spherical structures in adsorbed BFG films have also been previously observed in SEM images.[12a,d,e] These reports interpret these spheres as fibrinogen aggregates. The aggregates observed here are stable to imaging for at least 5 h, implying a robust structure. Upon initial inspection, the lower background region appears molecularly flat and could be interpreted as the HOPG substrate. However, as detailed below, images collected during BFG adsorption show that the background consists of a well-packed BFG monolayer. It is not clear from Figure 1C and D, however, whether the aggregates form on top of the initial BFG monolayer or if they are bound to the substrate surface and are embedded in the BFG monolayer.

An identical experiment was performed on a cleaved mica surface. Parts A and B of Figure 2 are representative topographic and lateral force images of freshly cleaved mica in PB. The topography of mica is atomically smooth, and the friction is constant over the surface. The structure of a BFG film formed on mica from a 50 μg/mL solution is illustrated in parts C and D of Figure 2. Although it is subtle, the presence of adsorbed BFG is indicated by an increase in the rms roughness of the surface from 0.087 nm for unmodified mica to 0.618 nm for Figure 2C. The BFG film exhibits a uniform topography and friction. With the imaging forces used here ($\leq$1 nN) we do not observe tip-induced displacement of the BFG, as has been illustrated previously.[28a] Unlike the film structure on hydrophobic HOPG, however, spherical aggregates do not exist in BFG films adsorbed to mica. It is clear from Figures 1 and 2 that the SFM-observed morphology of BFG films is influenced by the nature of the substrate.

Real-Time BFG Film Formation. To monitor the adsorption of BFG in real-time, our experiments were performed while either PB or BFG solution was flowing through the SFM fluid cell at a rate of 0.6−0.8 mL/min. Images collected during such an experiment at a cleaved HOPG surface are shown in Figure 3. Each image represents consecutive scans requiring ~50 s to complete. This is a sufficiently long time scale that the development of the BFG film can be monitored during a single image as well as through image to image comparisons. Figure 3A is the topographic image of the initial HOPG substrate collected in flowing PB. This image remained constant for ~4 min prior to the addition of BFG, illustrating the stability of imaging under flow conditions. Bovine fibrinogen solution was then added to the buffer reservoir and allowed to flow through the SFM fluid cell. Part B of Figure 3 is a topographic image collected as the slow scan axis advanced from bottom to top. Because the BFG has not yet reached the fluid cell, the lower portion of the image resembles the original substrate.

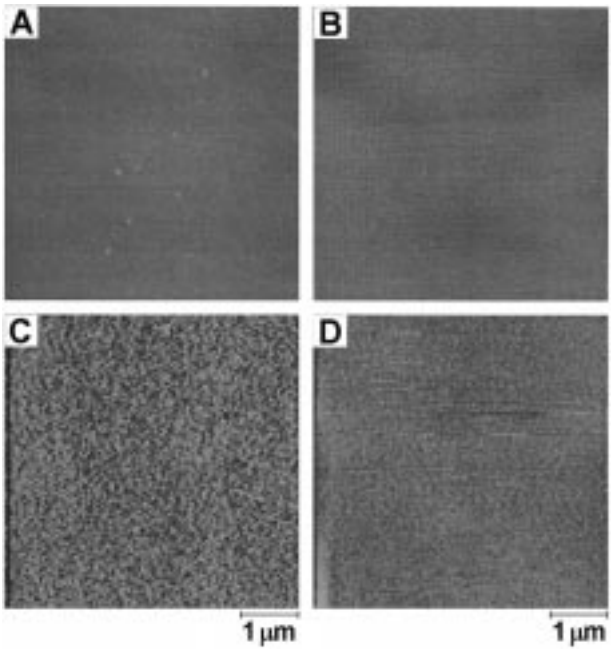

Figure 2. In situ SFM images of an unmodified mica substrate and a BFG film on mica. (A) 5×5 μm^2 topographic SFM image of cleaved mica in phosphate buffer (z-scale = 5 nm) and (B) corresponding lateral force image (z-scale = 0.1 V). (C) 5×5 μm^2 topographic image of a BFG film on mica adsorbed from a 50 μg/mL BFG solution for 30 min (z-scale = 5 nm) and (D) corresponding lateral force image (z-scale = 0.1 V).

The initial stages of BFG adsorption are observed in the top half of Figure 3B and appear as 3−4-nm increases in topography.[38] Although the accepted rodlike structure of BFG is not resolved in our images, this does not preclude that the initial adsorbed structures in Figure 3B are individual BFG molecules. However, because the SFM tip can artificially broaden the lateral dimensions of small structures, the actual size of these features is uncertain and it would be risky to identify them as single molecules. We thus designate these structures as clusters. The height of the clusters is inconsistent with any of the known dimensions of BFG (45 nm long × 9 nm wide) but is similar to the SFM-measured height of individual fibrinogen molecules adsorbed at a hydrophobic surface.[27a] The measured height reflects either a tip-induced compression of the surface-bound BFG or a diminished molecular dimension resulting from protein denaturation upon adsorption. The structure in the top right corner marked with arrow a is the nucleation of a BFG strand. For adsorption timing purposes, we define $t = 0$ as approximately halfway through Figure 3B with the image being complete at $t = 25$ s. The time scale is listed here simply as a means to track BFG film formation. We do not extract any kinetic information from these data.

Parts C and D in Figure 3 are topographic and lateral force images, respectively, of the ensuing downward scan. A higher density of larger clusters relative to those in Figure 3B is observed early, at the top of the image. A number of these clusters have lengthened into strands, and indeed the strand highlighted in Figure 3B (arrow a) appears to have grown in length and formed a branching

(37) McDermott, M. T.; Green, J.-B. D.; Porter, M. D. *Langmuir* **1997**, *13*, 2504−10.

(38) We do not report the lateral dimensions of any observed structures here because the well-known broadening effect of the SFM tip renders these measurements questionable.

(39) Ta, T. C.; Sykes, M. T.; McDermott, M. T. Manuscript in preparation.

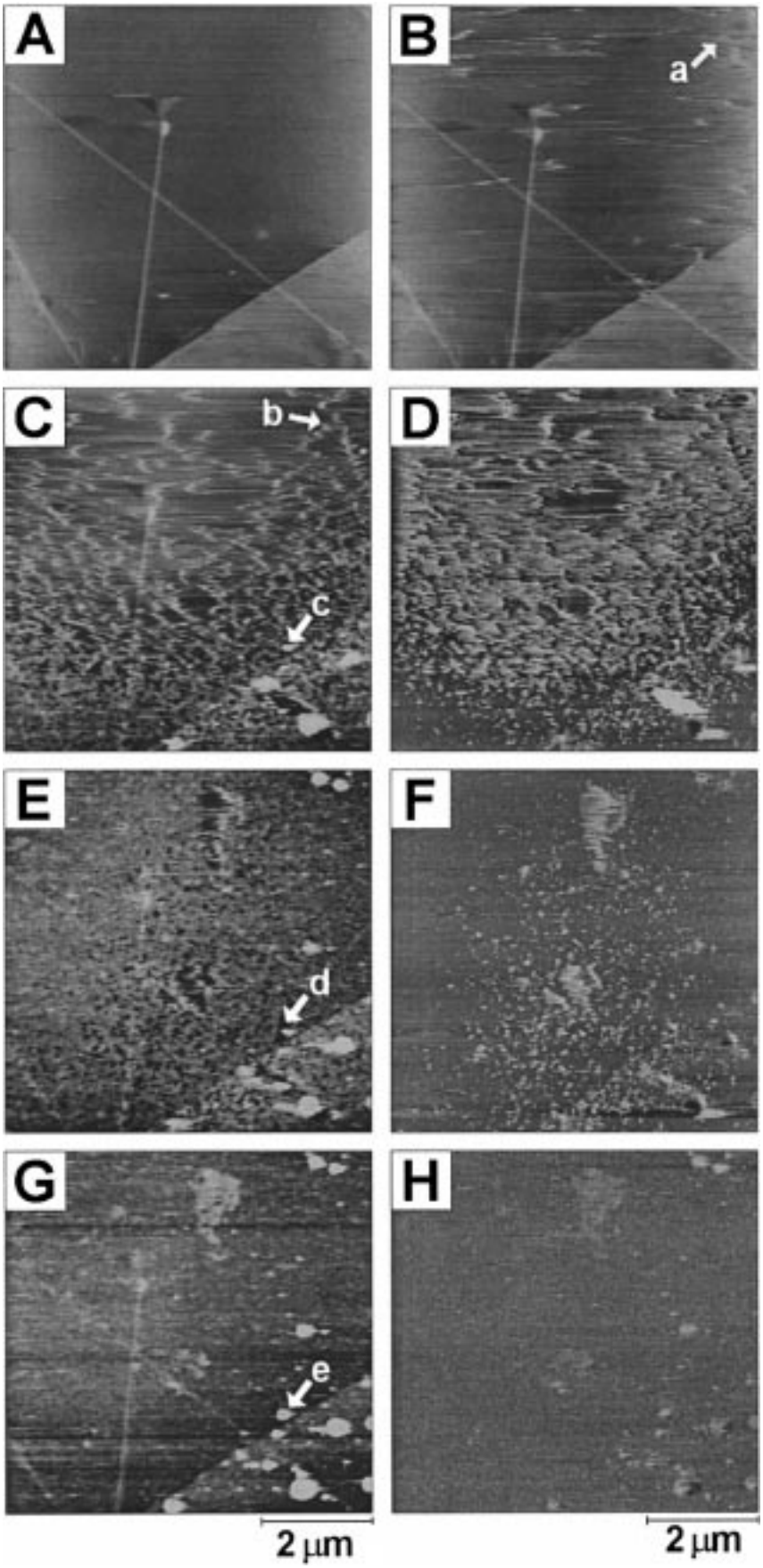

Figure 3. $6.6 \times 6.6\ \mu m^2$ consecutive SFM images of BFG film growth on HOPG monitored in real-time with continuous flow. Parts A and B are topographic images (z-scale = 10 nm). Parts C, E, and G are topographic images (z-scale = 10 nm), while parts D, F, and H are the corresponding lateral force images (z-scale = 0.2 V). For timing purposes the center of the scan in part B is defined as $t = 0$, as this is the point initial adsorption is observed. Parts C and D were captured 75 s after initial adsorption. Parts E and F correspond to 125 s, and parts G and H correspond to 225 s.

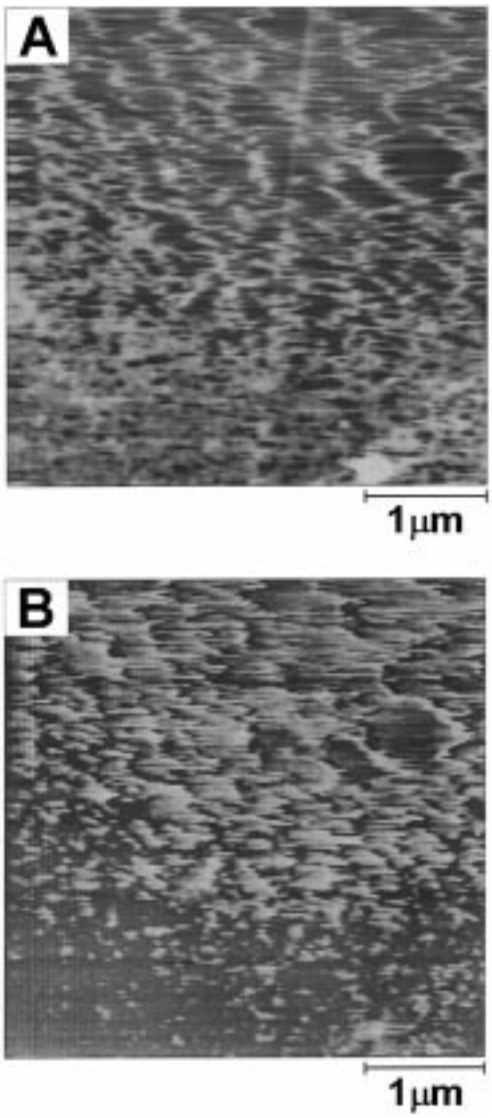

Figure 4. $4 \times 4\,\mu m^2$ (A) topographic and (B) lateral force images from a software zoom of the lower left corner of Figure 3C and D.

point (arrow b). The "streaks" apparent in Figure 3C and D imply that some tip-induced displacement of the protein strands is occurring at these early stages.[30] Within a few seconds, a denser network of strands has formed in the center portion of the images. This network finally merges to become a nearly completed BFG monolayer in the bottom region of Figure 3C and D. This is shown more clearly in Figure 4, which is a $4 \times 4\,\mu m^2$ expanded view (software zoom) of the lower left corner of Figure 3C and D. Note that the streaking is less significant as the network becomes more densely packed. Several strands are oriented perpendicular to the fast scan direction, indicating that the probe tip is not preferentially aligning the fully formed strands with the direction of the scan. The structure of the monolayer in the bottom portion of the images appears to be relatively densely packed with a few small defects apparent as depressions in the topography (Figures 3C and 4A). The low and constant frictional signal of the near-complete film that is observed in the bottom left corner of Figure 4B (and Figure 3D) implies a robust, crystalline-like architecture.[37] A tripping signal in the lateral force images is observed as the tip scans over the topographic defects in the near-complete monolayer. Also apparent in the bottom right corner of parts B and C of Figure 3 are several spherical aggregates similar to those observed in equilibrium films (Figure 1C and D).

A fibrinogen network has previously been observed in SEM images.[12c,f] Recent SFM studies have also noted the formation of a network structure at hydrophobic silicon and poly(tetrafluoroethylene).[27] The observation of a network early in the growth process in this work argues that significant intermolecular interactions are involved in BFG film formation on HOPG. We have also observed branched strands in SFM investigations of equilibrium BFG films on HOPG assembled from lower concentration solutions (e.g., 5 μg/mL).[39] A growth process driven by intermolecular interactions is consistent with an island mechanism whereby a monolayer forms via accretion of adsorbate at island edges via migration across the substrate surface. However, in contrast to the island growth mechanism, the BFG monolayer appears to develop via an increase in the density of the network strands through additional branching (Figure 4). Importantly, protein−protein interactions that develop during film formation will be retained and contribute to a robust final film structure.

There are no observable differences in the formation or final structure of the BFG layer near the location of the step defect at the lower right corner of the image area in Figure 4. The differences in reactivity between edge plane and basal plane HOPG are well-documented.[40] For example, the adsorption for quinones[40b] and dye molecules[41] is enhanced at defect sites relative to the basal plane due to the exposure of the higher reactivity edge plane at a step. Carbon biomaterials such as LTIC, which are utilized in prosthetic heart valves, exhibit a complex surface microstructure containing nanometer-sized domains of both edge plane and basal plane.[42] We have not noted preferential nucleation or growth at step defects, implying that BFG adsorption is not sensitive to the graphite microstructure. Thus, the well-defined surface of HOPG can be considered a model for the surface of less ordered carbon biomaterials such as LITC.

Further progress of the film formation is detailed in parts E−H of Figure 3. The topography and lateral force images of Figure 3E and F are the upward scan collected after Figure 3C and D and represent the film structure after 125 s. The basal plane surface is nearly completely covered with a well-packed layer of BFG, as is illustrated by a low and constant frictional response over the majority of the image in Figure 3F. Some pinhole defects in the film structure are observed in the topography and appear as localized increases in the lateral force. Two large defects are also apparent in the center and at the top of the images. A gradient in the density of the pinholes is evident with more defects present early in the scan. As time progresses, either the defect sites become occupied by solution-bound BFG molecules or the monolayer reorganizes to "heal" the defects, resulting in a lower defect density near the top of Figure 3E and F. The initial aggregates formed in the bottom portion of the image remain stable to imaging while aggregates have also formed coincident with the fully developed monolayer in the center and top of the image.

Parts G and H of Figure 3 are the topographic and lateral force images after 225 s and represent complete film

(40) (a) McCreery, R. L. In *Electroanalytical Chemistry*; Bard, A. J., Ed.; Marcel Dekker: New York, 1991; Vol. 17. (b) McDermott, M. T.; Kneten, K. R.; McCreery, R. L. *J. Phys. Chem.* **1992**, *96*, 3124−30.
(41) Ray, K., III; McCreery, R. L. *Anal. Chem.* **1997**, *69*, 4680−7.
(42) Bokros, J. C.; Lagrange, L. D.; Shoen, F. J. In *Chemistry and Physics of Carbon*; Walker, P. L., Jr., Thrower, P. E., Eds.; Dekker: New York, 1973; pp 103−262.

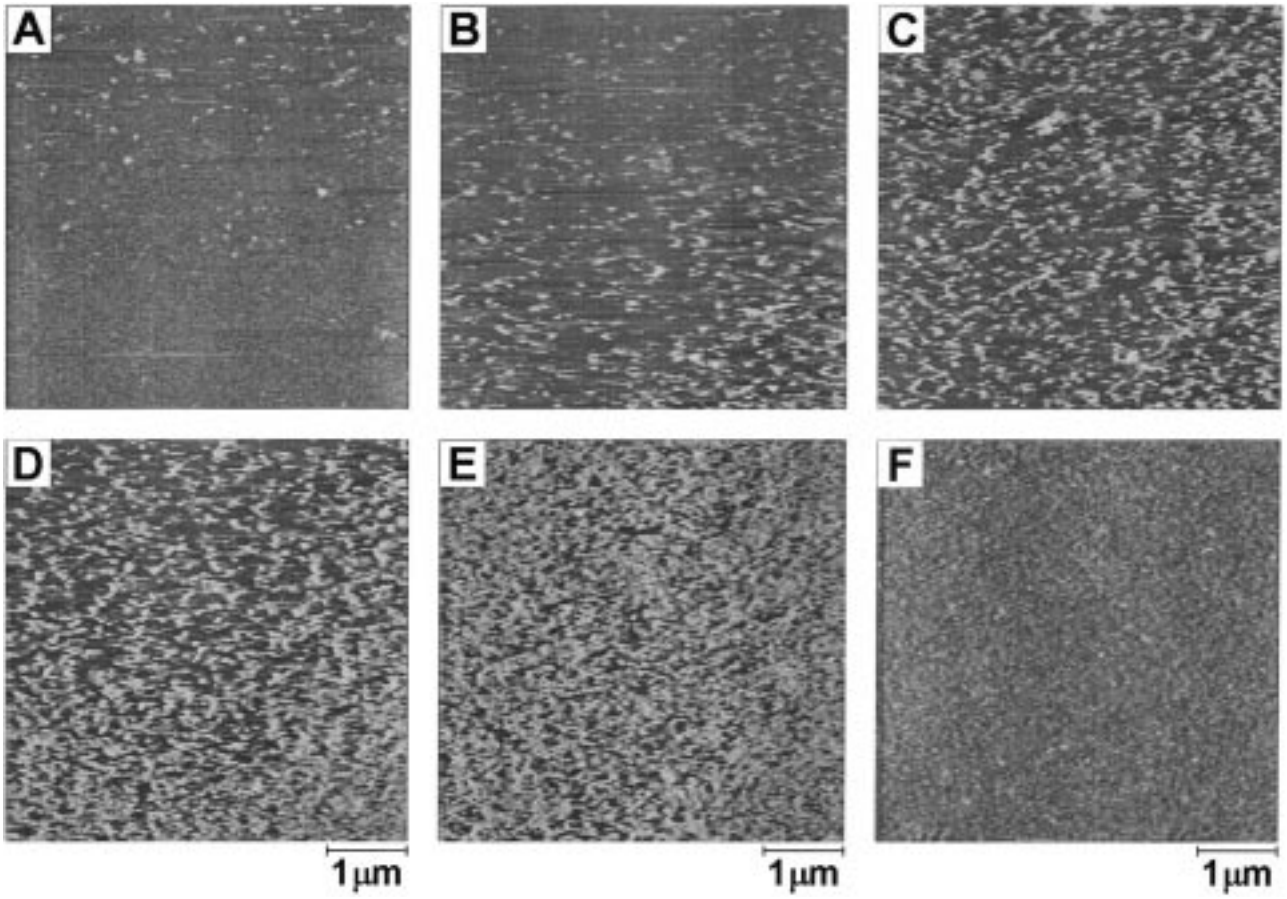

Figure 5. 5 × 5 μm^2 SFM images of BFG film growth on mica monitored in real-time with continuous flow. All images are topographic with a *z*-scale = 10 nm except for part A, where the *z*-scale = 5 nm. (A) Upward scan whereby we define $t = 0$ s as halfway through the scan. (B) Successive downward scan, with an elapsed time of 75 s. (C) Successive upward scan with an elapsed time of 125 s. (D) Successive downward scan with an elapsed time of 175 s. (E) Successive upward scan with an elapsed time of 225 s. (F) Upward scan with an elapsed time of 325 s.

formation. No significant changes in film structure were noted after this point, and multilayer adsorption was not observed. The pinhole defects observed in previous images have been completely "healed". Interestingly, the BFG molecules that have adsorbed in the larger defects observed in Figure 3E and 3F have apparently adopted a different conformation from the surrounding area, as indicated by a higher topography in Figure 3G and slightly higher friction in Figure 3H at these areas. We believe these larger defects are the result of the probe tip interfering with the monolayer formation, as we have not observed the variations in topography and friction apparent in parts G and H of Figure 3 in preformed films. We note that the tip also hinders the formation of the aggregates. While some spherical structures are apparent in Figure 3G, the density is much lower than that in Figure 1C. Subsequent imaging of the region outside the scan area in Figure 3 revealed aggregates at a density similar to that observed in Figure 1C. Although we note some tip interference during BFG film formation, the topography and friction of the monolayer in parts G and H of Figure 3 are identical to those of preformed films. Thus, we believe that the images in Figure 3 accurately reflect the actual film formation.

Careful inspection of the images in Figure 3 shows that aggregates initially form at the basal plane surface and become embedded in the surrounding close-packed monolayer. Arrow c in Figure 3C highlights the nascent growth of a single aggregate which is fully formed in Figure 3G (arrow e). In Figure 3C this aggregate appears to be located in a region where the monolayer is incomplete. Thus, a fully packed layer is not required for nucleation of the aggregates. In Figure 3E, the surrounding monolayer is more fully formed; however, a defect site remains apparent around the aggregate (arrow d), strongly arguing that the aggregate is associated with the basal plane substrate. In Figure 3G the monolayer is fully formed and has completely surrounded the aggregate (arrow e).[43] These observations thus support a model where a single BFG molecule (or a small group of BFG molecules) initially binds to the basal plane surface in a conformation that induces aggregation. The aggregates and monolayer form simultaneously, and the aggregates are ultimately embedded in a well-packed film.

In summary, our real-time observation of BFG film formation from single-component solutions indicates a mechanism involving the nucleation of small molecular clusters that assemble into branched strands. The branching of the two-dimensional network continues until a densely packed monolayer film results. Concurrently, localized three-dimensional growth occurs, leading to a dispersed array of aggregates that become embedded in the BFG monolayer.

Figure 5 shows the topographic images tracking BFG film formation at the mica−buffer interface. The lateral force images do not provide any additional information and are not included in this case. Figure 5A is the upward scan after PB containing BFG begins to flow through the

(43) In our ongoing investigations of aggregate formation as a function of concentration, we have also observed aggregates bound in film defects for films formed from lower concentration solutions.[39]

cell. Initially, individual clusters adsorb randomly across the mica surface. The height of these structures ranges from 4 to 6 nm, similar to those of the initial structures seen at HOPG. Parts B−E are consecutive scans following the initial adsorption noted in Figure 5A. The image resulting from the ensuing downward scan (Figure 5B) shows a homogeneous increase in the density of dispersed clusters especially near the bottom of the image where more time has elapsed. This trend continues throughout the intermediate stages of film growth until the bottom of Figure 5D, where the monolayer appears near complete. In some cases larger clusters are observed, but in general, the film growth on mica can be described by a uniform increase in the density of adsorbed BFG molecules or clusters. The formation of a network of strands on mica is not observed. The growth process observed in Figure 5 implies that the driving force for adsorbate−substrate nucleation is greater than that for the formation of protein−protein interactions. The lack of evidence for lateral interactions during film formation is in marked contrast to the growth process on HOPG. The formation of the film is complete in approximately 5 min, and the film is defect-free and appears to be well-packed. Multilayers or aggregates were not observed. The region outside the scan appears identical to the image area of Figure 5, indicating little interference of the tip.

Surfactant-Induced Elution Studies. It is clear from the observations presented above that BFG can form complete monolayers on both HOPG and mica. This is not surprising considering that several studies have shown that the nature of the substrate has little influence on the quantity of fibrinogen adsorbed.[5] In contrast, Figures 3 and 5 illustrate different growth mechanisms at each substrate. Differences in the formation of an adsorbed layer will likely be manifested in variations in the final film properties. One variation that is readily apparent is the film morphology on each substrate depicted in Figures 1 and 2. Another final film property that was evaluated is how tightly the BFG layer was bound to each substrate. The elution of surface-bound proteins by surfactant solutions is a well-accepted method for gauging adsorbate−substrate binding.[14d,44] We suspected that the BFG film would be more robust on HOPG compared to mica on the basis of the higher degree of intermolecular interactions involved in film formation.

Figure 6 presents the images of preformed films before and after exposure to a flowing SDS solution. Figure 6A is a $10 \times 10\ \mu m^2$ topographic image in PB of a BFG film formed at HOPG. Figure 6B is the corresponding topographic image in PB after the SDS solution was allowed to flow through the fluid cell.[45] The monolayer and aggregates are present in both images, implying that SDS has little affect on the film adsorbed at HOPG. This observation is consistent with recent results indicating a low susceptibility of fibrinogen adsorbed on LTIC to SDS elution.[31,32] Parts C and D of Figure 6 are $9 \times 9\ \mu m^2$ before and after images for an identical experiment on mica. As illustrated in Figure 6D, the SDS significantly displaces the monolayer from the mica surface. The large structure apparent on the right-hand side of Figure 6D is not related to the protein monolayer and is likely an impurity. These experiments provide compelling evidence that BFG monolayers are tightly bound to HOPG surfaces and only weakly interact with mica, as was predicted on the basis of the observed growth patterns. The significance

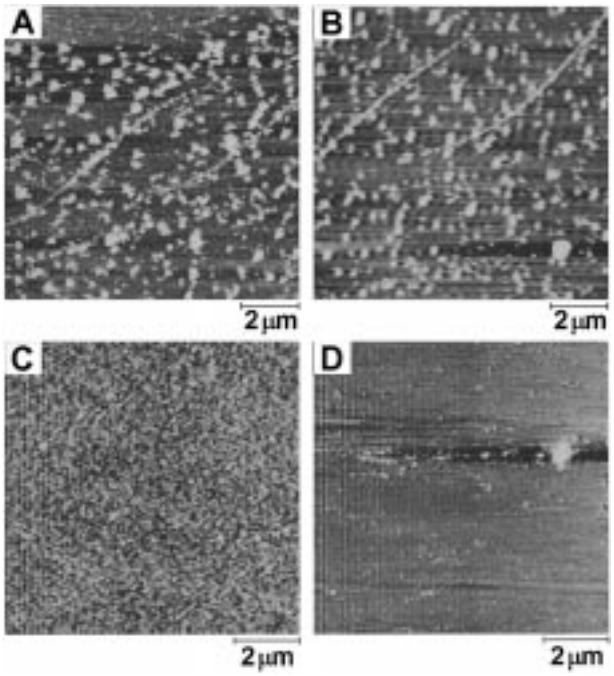

Figure 6. $10 \times 10\ \mu m^2$ SFM images. (A) Topographic (z-scale = 30 nm) image in PB of BFG film preformed on HOPG. (B) Topographic (z-scale = 25 nm) image in PB of BFG film on HOPG after 60 min of elution with 3% w/v SDS at a flow rate of 1 mL/min. (C) Topographic (z-scale = 5 nm) image in PB of a BFG film preformed on mica. (D) Topographic (z-scale = 7 nm) image of a BFG film on mica after 60 min of elution with 3% w/v SDS at a flow rate of 1 mL/min.

of this result stems from a previous report which correlated the amount of fibrinogen eluted with SDS with platelet binding.[14d] For example, fibrinogen that was more tightly bound to polymer surfaces exhibited a lower affinity for platelets than a loosely bound layer. Thus, because interfacial platelet aggregation is a key step in the formation of a blood clot, the biocompatibility of a surface may be influenced by how tightly it binds fibrinogen.

Structural Basis for Different Film Growth Mechanisms. Fibrinogen is a large protein (MW ~ 340 000 Da) which exists as a dimer with several molecular domains. Figure 7A shows a schematic of a BFG molecule highlighting the structural regions pertinent to the following discussion. A detailed discussion on the structure of each domain and the corresponding effect on adsorption has recently appeared.[4] The distal D domains are known to be hydrophobic with lower structural stability, allowing these regions to deform and maximize their contact area upon adsorption to hydrophobic surfaces. These domains also carry a −4 net charge. Two αC domains extend from each D domain and consist of the C termini of one of the three pairs of polypeptide chains that comprise BFG (i.e., the Aα chain). This domain contains both hydrophobic and hydrophilic regions and carries a net +2 charge. The αC domain is not directly involved in the polymerization of BFG to fibrin but may be involved in the branching and stabilization of fibrin.[4]

The results presented above point to a tightly bound BFG film on HOPG that features significant lateral interactions. A mechanism involving adsorbate−substrate binding through the D domain and intermolecular coupling through the αC domains is consistent with our observations. The hydrophobic D domains likely interact with the HOPG in a manner similar to that proposed for hydrophobic binding of FG to LTIC.[31a] This situation is depicted in Figure 7A. Another possibility resulting in

(44) Bohnert, J. L.; Horbett, T. A. *J. Colloid Interface Sci.* **1986**, *111*, 363−77.

(45) There was no evidence to indicate that any SDS was adsorbed to the probe tip after flushing the cell with PB.

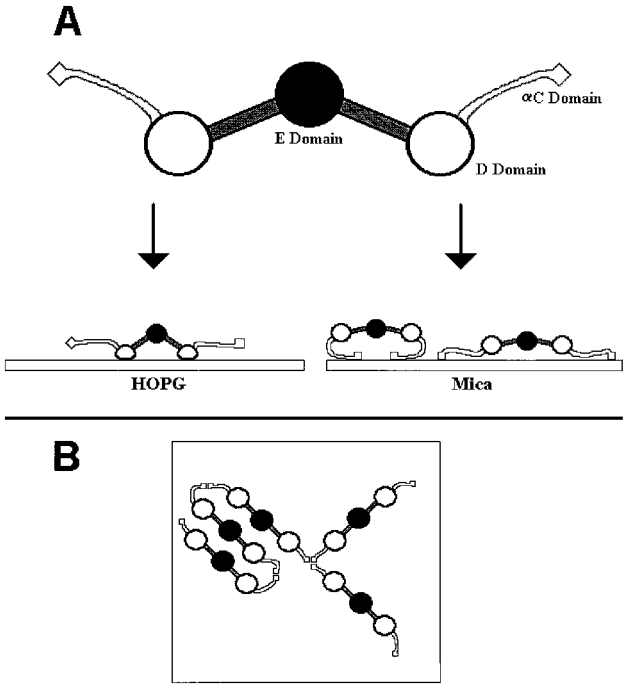

Figure 7. (A) Schematic representation of a proposed model for (A) fibrinogen adsorption to HOPG and mica and (B) fibrinogen network formation on HOPG.

an identical final outcome involves an initial relatively weak hydrophobic interaction between the graphite surface and the hydrophobic region of the αC domain. This mechanism is attractive on the basis of the high flexibility of this domain that permits high collision frequencies.[4] A stronger hydrophobic binding between the D domains and the surface follows the initial interaction, thus freeing the αC domains to interact elsewhere.

The results from several studies point to a strong tendency of the αC domain to interact with other αC domains both intra- and intermolecularly.[5] Several reports have provided evidence that the αC domains contain complementary sites which bind intramolecularly to form a superdomain[46] observed by SEM.[47] These sites also provide the pathway for enhanced intermolecular interactions. We propose that the surface-bound BFG network observed here and elsewhere[12c,f,27] forms from the coupling of αC domains on adjacent molecules. Branching would occur via interactions between multiple αC domains, as illustrated in Figure 7B. The combined effect of hydrophobic adsorbate−substrate binding through the D domain and strong lateral interactions results in a crystalline-like monolayer which is tenaciously bound to carbon materials. We note that interactions between αC domains on adjacent proteins also provide a viable pathway for aggregate formation.

The relatively weak adsorption of BFG to mica surfaces as evidenced by SDS elution implies a much different binding mechanism relative to that for HOPG. The hydrophilic mica surface is unlikely to induce significant hydrophobic interactions with domains on BFG. Following the arguments presented above, the lack of any significant evidence for intermolecular interactions in the images detailing film growth in Figure 5 suggests little coupling of αC domains in adjacent molecules. The isoelectric point of mica ranges between 3 and 3.5.[48] Thus in addition to being hydrophilic, the surface of mica is negatively charged at a pH of 7.4 and could interact electrostatically with the positively charged αC domains of BFG. These domains would then be unavailable to form lateral intermolecular interactions. It has recently been predicted that interactions between a αC domain and a surface should not be strong on the basis of a low degree of hydrophobicity and a low net charge.[4] Electrostatic interactions are also expected to be mediated by ionic species in the solution.[31b] In addition, adsorbed BFG has been readily eluted with SDS when bound to a surface only through its αC domain.[5] Thus, a mechanism involving the electrostatic binding of BFG to mica through the αC domains, as depicted in Figure 7A, is consistent with our observations.

Conclusions

We have shown that the morphology of fibrinogen films depends on the nature of the substrate. Fibrinogen films adsorbed to HOPG are composed of uniformly distributed aggregates embedded in a well-packed monolayer. A fully formed monolayer is observed on mica with no evidence of aggregates. SFM real-time monitoring of fibrinogen film formation has provided insights into the growth mechanism at each surface. The growth of BFG films on HOPG proceeds via network formation and propagation and involves lateral interactions between adsorbates. The final film structure is the result of strong intermolecular interactions and tight binding to the surface. These properties are reflected in a high resistance to elution by SDS. We propose that BFG binds to the graphite hydrophobically through the D domains and that lateral interactions form through the αC domains. On mica surfaces, BFG film growth involves a homogeneous increase in nucleation sites, indicating that mica−BFG interactions are stronger than any intermolecular interactions. The resulting film is easily eluted by SDS. An electrostatic interaction between the positively charged αC domains and the negatively charged mica is consistent with our observations.

The results of this study reflect the behavior of BFG films formed from single-component solutions (i.e., containing only BFG). The presence of other proteins and components will strongly influence film structure at true blood−biomaterial interfaces.[1,28b] We believe that our experiments here provide the basis for monitoring competition phenomena during the formation of protein films from complex, multicomponent solutions such as serum and plasma. Experiments to this effect are underway.

Acknowledgment. This work was supported by the Natural Sciences and Engineering Research Council of Canada (NSERC) and the Department of Chemistry, University of Alberta. We thank P. K. Hansma for useful discussions concerning imaging under flow.

LA9712348

(46) (a) Doolittle, R. F. In *BFG, thrombosis, coagulation and BFGrinolysis*; Liu, C. I., Chien, S., Eds.; Plenum Press: New York, 1990; p 25. (b) Medved, L. V.; Gorkun, O. V.; Privalov, P. L. *FEBS Lett.* **1983**, *160*, 291−5.

(47) Rao, S. P. S. *J. Mol. Biol.* **1991**, *222*, 89.

(48) Reynders, P. Personal communication.